International Journal of Climatology

International Journal of Climatology | RMetS

RESEARCH ARTICLE OPEN ACCESS

Scaling of Short-Duration, Summer Rainfall Event Temporal Profiles With Warming Over Great Britain

Alexandra Seawell[1] | Hayley J. Fowler[1,2] | Stephen Blenkinsop[1,2] | Caspar J. M. Hewett[1] | Roberto Villalobos Herrera[1,3] | Marie Hundhausen[4] | Haider Ali[1]

[1]School of Engineering, Newcastle University, Newcastle upon Tyne, UK | [2]Tyndall Centre for Climate Change Research, Newcastle University, Newcastle upon Tyne, UK | [3]School of Civil Engineering, University of Costa Rica, San José, Costa Rica | [4]Institute of Meteorology and Climate Research Troposphere Research (IMKTRO), Karlsruhe Institute of Technology (KIT), Karlsruhe, Germany

Correspondence: Alexandra Seawell (a.seawell2@newcastle.ac.uk)

Received: 18 November 2025 | **Revised:** 15 April 2026 | **Accepted:** 24 April 2026

Keywords: Clausius-Clapeyron | convection-permitting model (CPM) | convective rainfall | dewpoint temperature | flash flooding | rainfall temporal profile | sub-hourly precipitation | temperature scaling

ABSTRACT

The relationship between extreme rainfall and temperature, known as temperature scaling, is widely used to understand changes in rainfall characteristics under a warming climate. While most previous studies have focussed on fixed-duration intensities or event totals, this study examines how different aspects of the rainfall temporal profile respond to temperature. Specifically, we focus on temperature scaling of total event depth, maximum sub-hourly intensity and measures of profile concentration and loading. Using both sub-hourly rain gauge data across Britain and 10-min output from a convection-permitting climate model (CPM) for present and future climates over southern England and Wales, we analyse short-duration, summer rainstorms. Results show that total rainfall depth increases with temperature, with higher quantiles approaching Clausius-Clapeyron (CC) scaling rates of 6–7%°C^{-1}. However, changes are unevenly distributed within the rainfall event temporal structure. Maximum sub-hourly intensities scale more strongly than total event depth, with upper quantiles reaching 7–11%°C^{-1}, indicating pronounced intensification of short-duration rainfall extremes at high temperatures. Accumulation of 50% of the rainfall event volume was found to occur over a shorter fraction of the storm duration and earlier in the storm duration, indicating rainfall events are more concentrated and more front-loaded at higher temperatures, with both scaling at rates of 1–2%°C^{-1}. These results suggest that future summer rainstorms will not only deliver greater overall rainfall in a warming climate, but also produce more intense and earlier bursts of precipitation, heightening flash flood risk. Disregarding these temporal shifts may lead to underestimation of flood hazards and misrepresentation of climate change impacts in hydrological modelling and infrastructure design.

1 | Introduction

Flash flooding poses a major societal risk, causing damage to infrastructure, transport disruption and loss of life. Its impacts are exacerbated by rapid onset and the potential to occur almost anywhere, particularly in urban and rapid response catchments (Jonkman 2005; Doocy et al. 2013; Hu et al. 2018; Archer and Fowler 2021; Dale 2021). Anticipating how rainfall characteristics will evolve under climate change is therefore critical for effective flood management and adaptation. A widely used diagnostic is the relationship between rainfall intensity and temperature, known as temperature scaling, which infers how rainfall extremes may respond to warming. This approach builds on the Clausius-Clapeyron (CC) relationship, which states that the atmosphere's moisture-holding capacity increases by about 6–7% per 1°C rise in temperature (Trenberth 1999; Allen and Ingram 2002). The effect of a warmer, wetter global atmosphere on precipitation is complex and varies at different locations. In

the UK, climate model projections indicate that winters will be warmer and wetter and summers hotter and drier; however, despite the overall summer drying trends, the rainfall that does occur will show increased intensity of heavy summer rainfall events (Intergovernmental Panel on Climate Change 2021; Kendon et al. 2021; Met Office Hadley Centre 2022). To broaden understanding of future rainfall, research efforts have investigated the relationship of rainfall with temperature, where the 'apparent scaling' of rainfall with daily temperature variability is used as a proxy for 'climate scaling' in a warmer future (Fowler et al. 2021).

Empirical studies reveal, however, that apparent scaling is highly variable. While some studies report CC-like increases (Chan et al. 2015, 2016), others find super-CC (Kendon, Stratton, et al. 2019; Ali, Fowler, et al. 2021; Ali, Peleg, and Fowler 2021; Ali et al. 2022) and sub-CC (Ali et al. 2018; Pumo et al. 2019), and even negative scaling (Hardwick Jones et al. 2010; Utsumi et al. 2011; Ali and Mishra 2017; Kendon, Stratton, et al. 2019; Ali et al. 2022). A peak-like relationship, with rainfall intensity rising then declining beyond a temperature threshold, is also common (Lenderink and van Meijgaard 2008; Hardwick Jones et al. 2010; Wang et al. 2017; Pan et al. 2019; Pumo et al. 2019). Such variation reflects differences in rainfall type, with stratiform rainfall generally following CC scaling, whereas convective storms can exceed CC rates due to enhanced latent heating and stronger updrafts (Trenberth et al. 2003; Lenderink and Van Meijgaard 2010; Singleton and Toumi 2013). Apparent super-CC scaling may also result from mixing storm types, as warmer conditions favour more convective events (Berg et al. 2013; Da Silva and Haerter 2025; Xie et al. 2025). Scaling rates also depend on season (Lenderink and van Meijgaard 2008; Blenkinsop et al. 2015; Pan et al. 2019; Pumo et al. 2019), weather type (Blenkinsop et al. 2015; Magan et al. 2020), region (Utsumi et al. 2011; Panthou et al. 2014; Ban et al. 2015; Molnar et al. 2015; Prein et al. 2016; Peleg et al. 2018; Van de Vyver et al. 2019; Ali, Fowler, et al. 2021; Ali, Peleg, and Fowler 2021) and urbanisation (Pan et al. 2019), which affect the occurrence and intensity of convective activity.

Methodological choices further affect scaling estimates. Steeper gradients are generally found for higher rainfall quantiles (Lenderink and van Meijgaard 2008; Hardwick Jones et al. 2010; Singleton and Toumi 2013; Park and Min 2017; Kendon, Stratton, et al. 2019) and shorter accumulation periods (Lenderink and van Meijgaard 2008; Hardwick Jones et al. 2010; Singleton and Toumi 2013; Panthou et al. 2014; Park and Min 2017; Kendon, Stratton, et al. 2019; Hundhausen et al. 2024). Data quality, gauge pooling and spatial resolution also influence results (Molnar et al. 2015; Ali, Fowler, et al. 2021; Ali, Peleg, and Fowler 2021; Ali et al. 2022). High resolution convection-permitting models (CPMs) better capture convective extremes than regional or global models (Kendon, Stratton, et al. 2019). Statistical techniques, such as binning versus quantile regression, introduce additional variation (Ali et al. 2022). Dewpoint temperature is now preferred over air temperature as a physically meaningful predictor, since it directly represents atmospheric moisture availability (Lenderink et al. 2011; Barbero et al. 2018; Ali, Fowler, et al. 2021), being a measure of atmospheric moisture translated to temperature through the CC relationship. In the UK, ensemble climate model projections indicate an average increase in dewpoint temperature of 2.5°C–4.0°C between baseline (1981–2000) and future (2061–2080) simulations (Kendon, Fosser, et al. 2019).

While early work focused on fixed-duration accumulations (e.g., daily, hourly), recent studies have shifted to event-based analyses, examining (near) continuous rainfall events separated by dry intervals (Panthou et al. 2014; Molnar et al. 2015; Pan et al. 2019; Najibi et al. 2022). This enables assessment of storm characteristics, such as total depth, duration, and maximum intensity, that are directly relevant for hydrological impacts, such as flash flooding (Berg et al. 2013). For example, events with concentrated temporal profiles, where much of the rainfall occurs within a short time, have been linked to severe urban flooding (Chen et al. 2015; Lana et al. 2020). Understanding event profile change with temperature is therefore crucial for improving flood risk projections.

Recent work highlights that scaling affects not only storm totals or peak intensities, but also rainfall timing within storms. Wasko and Sharma (2015) found that the most intense fractions of storms scale positively with temperature, while the weakest fractions scale negatively. Subsequent studies in the UK and USA reported similar behaviour (Fadhel et al. 2018; Hettiarachchi et al. 2018). Visser et al. (2023) introduced the "D_{50}" metric, representing the time within a storm by which 50% of the rainfall has occurred, and showed that storms across Australia become increasingly front-loaded with temperature increases. Global satellite analyses further reveal that higher temperatures tend to shorten, shrink and front-load low-latitude storms (Ghanghas et al. 2024). Together, these results suggest that warming may alter both the intensity and timing of rainfall within events, increasing flash flood potential.

In the UK, summer rainfall is dominated by convective storms (Blenkinsop et al. 2015; Rico-Ramirez et al. 2015), which are more temperature-sensitive than stratiform systems (Lenderink and Van Meijgaard 2010; Blenkinsop et al. 2015). Extreme sub-daily intensities have been shown to be greatest in southern regions during summer due to convective dominance (Blenkinsop and Fowler 2014; Blenkinsop et al. 2015, 2017; Allan et al. 2016). UKCP18 climate projections indicate average summer temperatures could rise by up to 5.4°C by 2070 (Lowe et al. 2019), with more frequent and intense downpours (Kendon et al. 2014; Met Office Hadley Centre 2022).

This study investigates how key characteristics of summer short-duration rainstorms: total depth, peak intensity, concentration and temporal loading, scale with dewpoint temperature. We analyse sub-hourly rain gauge data across Great Britain alongside 10-min CPM output for southern England and Wales, comparing present (1997–2009) and future (~2100 RCP 8.5) climates. By focussing on convective-type events, we provide new insight into how rainfall temporal profiles may evolve under warming. To our knowledge, this is the first study to examine profile-based scaling metrics using both observed and CPM-simulated rainfall in the UK, with direct implications for design storm estimation and flash flood adaptation under climate change.

The remainder of this paper is organised as follows: Section 2 describes the study region, datasets, rainfall indices and

methodology. Section 3 presents the results, followed with discussion and conclusions in Sections 4 and 5, respectively.

2 | Data and Methods

2.1 | Data

Rainfall events were identified using the method of Hundhausen et al. (2025), defining independent events as continuous rainfall $\geq 0.01\,\text{mm}\,\text{h}^{-1}$ with a minimum depth of 5 mm and duration ≥ 1 h, separated by a minimum 7.5 h 'dry' interval, termed the interarrival period, which has < 1 mm of rainfall. Allowing this minimal amount of rainfall in the interarrival period prevented the inclusion of long events with a large dry fraction by discounting minor precipitation peaks that were isolated from the main events (1 mm rainfall adjoining a main event was included within the event). Although spatial independence was not enforced, this is unlikely to affect results, as summer storms are small in scale and weakly correlated beyond ~10 km (Blenkinsop et al. 2017). Events observed at multiple gauges may differ in characteristics, thereby capturing spatial variability.

Sub-hourly rainfall data (5- and 15-min) from 1299 gauges across Great Britain were obtained from the Environment Agency, Natural Resources Wales (NRW) and the Scottish Environment Protection Agency (SEPA), with records extending from 1962 to 2018 and additional data for 1009 gauges to 2020. The 5-min rainfall was resampled to 15-min rainfall for analysis. All data underwent quality control following Villalobos-Herrera et al. (2022). Quality-controlled datasets substantially improve scaling robustness (Ali et al. 2022). Ali et al. (2022) reported higher and more consistent scaling rates for the Global Subdaily Rainfall (GSDR) data after quality control, with all gauges showing positive scaling of the 99th quantile (q99) hourly rainfall and over half exceeding CC expectations.

The observed rainfall events were paired with temperature data from ERA5-Land reanalysis (Copernicus Climate Change Service (C3S) 2019) at 0.25° resolution and hourly frequency. For each event, 2 m air and dewpoint temperatures were extracted at 1 and 3 h prior to onset; within the dry interarrival period, to avoid precipitation-induced cooling and humidity biases. ERA5-Land provides a reliable representation of near-surface moisture conditions over the UK (Ali, Peleg, and Fowler 2021). This paper presents results from dewpoint temperature (although results from air temperature are included in the Supporting Information Section S3).

Modelled events are obtained from the 1.5 km convection-permitting version of the Met Office Unified Model (MetUM) (Kendon et al. 2012, 2014), developed under the CONVective EXtremes (CONVEX) project. The CPM explicitly represents deep convection and reproduces the dynamical structures and life cycles of convective storms (Kendon et al. 2012, 2014; Chan et al. 2014) more realistically than convection-parameterized regional models, which tend to overproduce light rainfall (Stephens et al. 2010; Wilkinson et al. 2013).

The CONVEX CPM domain covers southern England and Wales and is driven by a 12-km regional climate model (RCM) version of the MetUM covering Europe, nested within a 60-km global climate model (GCM) (Kendon et al. 2014). Simulations span 13-year present (1997–2009) and future (~2100, under RCP 8.5) summer (JJA) periods. Outputs include 10-min rainfall, 1.5 m hourly air temperature and 3-h specific humidity. No significant temperature trends were detected within each 13-year time-slice.

Rainfall events and their paired air temperature and specific humidity were extracted from the CPM time-slices, using the same event definition as for observations. Dewpoint temperature was computed from air temperature and specific humidity using equations for saturated vapour pressure, partial vapour pressure and relative humidity following Bolton (1980), Lawrence (2005) and Cai (2019) (see Supporting Information Section S1). Previous analyses of sub-daily rainfall scaling in the UK to date, have used both observational (Blenkinsop et al. 2015) and the CONVEX CPM data (Chan et al. 2015, 2016), but focussed on fixed duration rainfall intensities or total event rainfall; here we focus on full rainfall events and their temporal characteristics.

2.2 | Pooling Criteria

A spatial pooling scheme was applied to ensure sufficient sample sizes for robust scaling analysis, noting that pooled results tend to yield slightly lower scaling rates than single sites due to spatial averaging of local dynamics. Previous comparisons show pooled scaling rates are typically 0.2 to $0.3\%\,^{\circ}\text{C}^{-1}$ lower than single-site estimates, with regional pooling shifting results from super-CC to predominantly CC behaviour (Ali, Fowler, et al. 2021; Ali et al. 2022).

Two pooling strategies were used for the rain gauge data: (1) a single nationwide pooling ("all-raingauges") and (2) regional and elevation-based subsets to capture climate variability and avoid artificially steepened scaling from combining gauges with differing precipitation mechanisms (Visser et al. 2021) or flattened scaling curves due to differing dewpoint regimes (Ali, Fowler, et al. 2021). Regional pooling followed the UK extreme hourly rainfall regions defined by Darwish et al. (2021) (Figure 1). Western regions, dominated by frontal and orographic rainfall and enhanced oceanic moisture advection, contrast with the more convective regimes of the south and east (Hand et al. 2004; Jones et al. 2014; Blenkinsop et al. 2017; Darwish et al. 2018, 2021). Elevation from the Ordnance Survey Terrain 50 digital terrain model was used to separate gauges above and below 400 m above sea level as high altitudes have lower dewpoint than lower altitudes (Ali, Fowler, et al. 2021).

Modelled events were analysed for the full CONVEX domain within southern England and Wales (areas overlying the ocean, Ireland and France were excluded) and west–east regional subdivision. Sensitivity tests repeated the rain gauge scaling using only gauges within the model domain and overlapping years (1997–2009). As regional and temporal subsets produced similar patterns, only results for the full model domain and national rain gauge pooling are presented here. Model scaling was also evaluated for the future simulations to assess the persistence of present-day relationships.

2.3 | Scaling Calculation

Four properties of the rainfall event were analysed: total depth, maximum sub-hourly intensity, D_{50} (a measure of rainfall timing within the event duration), and PW_{50} (a measure of rainfall concentration over the event duration). Table 1 describes the statistics calculated for each rainfall event, with a schematic illustration provided in Figure 2. The depth and maximum intensity were calculated for the original rainfall profile, while the PW_{50} and D_{50} values were calculated from the profile normalised over 100 time steps.

Scaling analysis was performed for precipitation events with dewpoint temperatures above 5°C, to remove anomalous outliers. The outlier events were not regionally clustered and corresponded to freezing or near-freezing conditions.

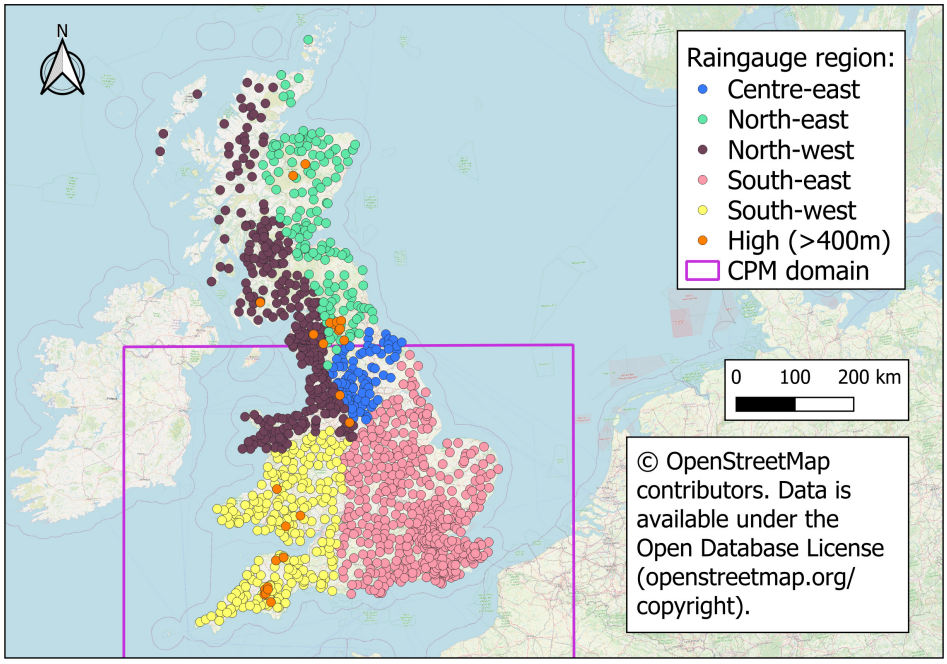

FIGURE 1 | Rain gauge pooling groups reflecting British rainfall characteristics shown by the five Darwish et al. (2021) regions in different colours, excluding rain gauges above 400 mAOD which are shown in orange. The CONVEX CPM model domain is indicated by the purple rectangle, although areas overlying the ocean, Ireland and France were excluded from analysis. [Colour figure can be viewed at wileyonlinelibrary.com]

TABLE 1 | Results analysis metrics.

Statistic	Description
Depth (mm)	The total event rainfall depth (volume of event).
Duration-50, or D_{50} (%)	Proportion of event duration elapsed when 50% of the total rainfall has occurred (Visser et al. 2023). Smaller values indicate front-loaded storms, where more rainfall occurs early in the event, while larger values indicate back-loaded storms, with more rainfall occurring later. For example, a D_{50} of 10% represents a strongly front-loaded storm, while 90% denotes a back-loaded storm.
Intensity maximum (mm/time-step)	The maximum rainfall intensity across all time-steps of the event. For rain gauge data, the time-step is 15 min; for the CONVEX CPM data it is 10 min.
Peakwidth-50, or PW_{50} (%)	The shortest proportion of the event duration during which 50% of the total rainfall occurs (M. Hundhausen, pers. comm.). This metric quantifies rainfall concentration. Smaller values indicate a more concentrated burst within the event, while larger values mean rainfall is more spread-out. For example, a PW_{50} of 10% means that half of the total rainfall occurs within 10% of the event duration, that is, a highly concentrated burst, whereas PW_{50} of 50% indicates fairly uniform rainfall across the event, while PW_{50} of 90% suggests significant rainfall in the early and late part of the event with gradual rainfall in-between, such as a double-peaked event.
Normalised cumulative profile (–)	Event time series, for which the cumulative rainfall and event duration were each normalised to a value of 1.0.

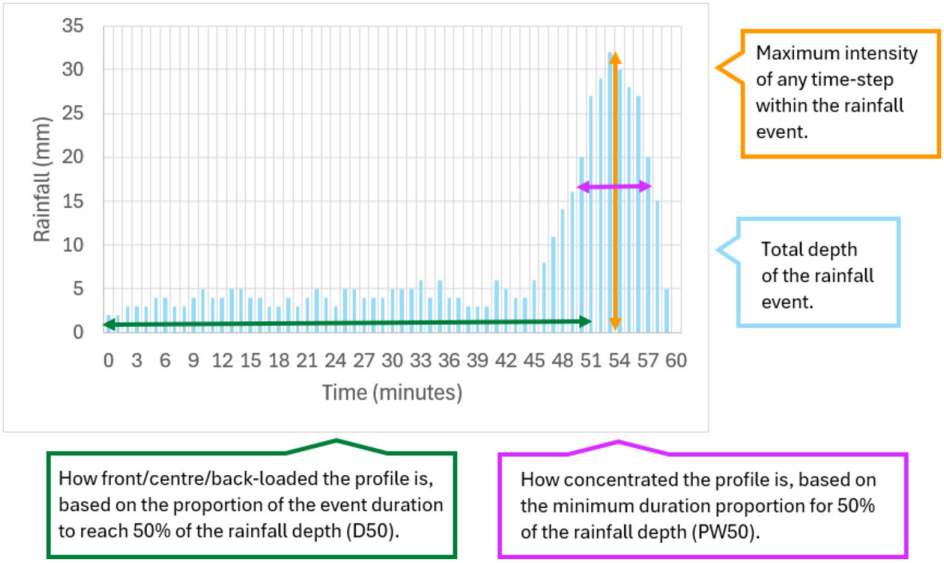

FIGURE 2 | Schematic of analysis metrics for rainfall events: Event depth, maximum intensity, peakwidth-50 (PW_{50}) and duration-50 (D_{50}). This is an imaginary profile, but it would have a D_{50} of 94% and PW_{50} of 5%. [Colour figure can be viewed at wileyonlinelibrary.com]

Three different scaling techniques were evaluated: equal-width binning (Lenderink and van Meijgaard 2008), equal-number binning (Hardwick Jones et al. 2010), and quantile regression (Wasko and Sharma 2014). In both binning methods a linear relationship between rainfall quantiles and temperature bins is fitted using ordinary least squares. Equal-width binning divides the temperature range into overlapping 2°C windows at 1°C intervals, to reduce sensitivity to arbitrary bin boundaries (Lenderink and Van Meijgaard 2010). Bins containing fewer than 100 samples were excluded to avoid instability in scaling gradients. Equal-number binning maintains constant sample size per bin but has variable temperature windows. Both binning approaches were implemented using Python's sklearn linear regression model (Pedregosa et al. 2011). Quantile regression fits a linear relation directly to the full dataset without binning. It minimises absolute, rather than squared, errors and applies asymmetric penalties for over- and underprediction, making it less sensitive to outliers and sample size (Wasko and Sharma 2014). The quantile regression approach was implemented using Python's Statsmodels quantreg function (Skipper and Perktold 2010).

The linear regression was applied to the log-transformed values of each rainfall metric at a given quantile, for example:

$$\log(q99) = \alpha + \beta T \tag{1}$$

where q99 is the 99th (or other) quantile of either rainfall depth, maximum intensity, PW_{50} or D_{50}, α is the regression intercept, β the regression slope and T is dewpoint temperature or air temperature. The scaling factor was estimated using an exponential transformation of the regression slope coefficient, for example:

$$\frac{\partial q99}{\partial T} = 100 * (\exp(\beta) - 1) \tag{2}$$

For rainfall depth and maximum intensity, quantiles represent event magnitude, with the 50th, 95th and 99th percentiles calculated to capture increasingly extreme events. For PW_{50} and D_{50}, quantiles describe event shape so are evaluated across the range of percentiles at regular intervals: the 10th, 30th, 50th, 70th and 90th percentiles, to assess how different temporal profile shapes scale with temperature.

Previous studies have shown that mixing events of different durations (Visser et al. 2021; Najibi et al. 2022), or rainfall types (Berg and Haerter 2013) can influence scaling rates. Although this study selects only summer events, some statistical mixing of stratiform and convective rainfall may remain (Da Silva and Haerter 2025). However, Hand et al. (2004) showed that all UK extreme rainfall events of < 5 h are predominantly convective. Thus, to minimise the effects of such mixing, events were classified into three duration categories:

- < 3 h (predominantly convective);
- 3–6 h (mixed convective and stratiform);
- 6–24 h (largely non-convective).

Events exceeding 24 h were excluded as they are unlikely to be primarily convective.

3 | Results

3.1 | Overview of Scaling

3.1.1 | Frequency of Rainfall Events

Because the CPM is driven by RCM and GCM boundary conditions, its simulated rainfall arises from physically-based processes that reproduce the climatological statistics of a given period rather than individual observed events. To evaluate realism, the frequency of simulated CONVEX CPM rainfall events was compared with observations. Although the CPM produces a greater total number of events (as all land grid cells are included), the present-day simulated event frequency per grid cell is approximately 86% of the observed frequency per gauge (Table 2). In the future time-slice, event frequency declines

markedly to about 50% of the present-day value, indicating longer dry intervals between summer rainfall events—consistent with projections of a warmer and drier UK summer climate (Kendon et al. 2014).

Changes in event frequency with temperature were examined using histograms for five equal-number temperature bins. Figure 3 shows event frequency as a function of dewpoint temperature. In both observations and the CPM present-day simulation, the proportion of short-duration events increases with temperature; a pattern also evident in the future simulation. This relationship occurs across all event profile types (front-, centre- and back-loaded) but is most pronounced for front-loaded storms.

TABLE 2 | Frequency of rainfall events from rain gauge observations (1997–2009) and CONVEX CPM simulations for the present-day (1997–2009) and future (~2100, RCP 8.5) 13-year periods.

	Number of rainfall events	Number of gauges or grid cells	Events per gauge or grid cell
Rain gauge observations	55,505	361	153.8
CPM present-day	6,077,291	45,787	132.7
CPM future	3,121,118	45,787	68.2

3.1.2 | Comparison of Scaling Techniques

Although equal-width binning and quantile regression are more sensitive to temperature ranges with limited sample sizes (see Supporting Information Section S2), the overall regression slopes for all three methods are broadly consistent (Figure 4 panels (a) and (b)). Consequently, results are presented using the equal-width binning approach to enable discussion of the detail of the quantile's behaviour. Additionally, scaling rates are consistently higher with dewpoint than with air temperature for precipitation events of equivalent duration (Figure 4 panels (c) and (d)).

The largest variations in scaling occur between the three storm duration groups. Events lasting < 3 h and 3–6 h have similar scaling rates, whereas 6–24 h events show markedly lower

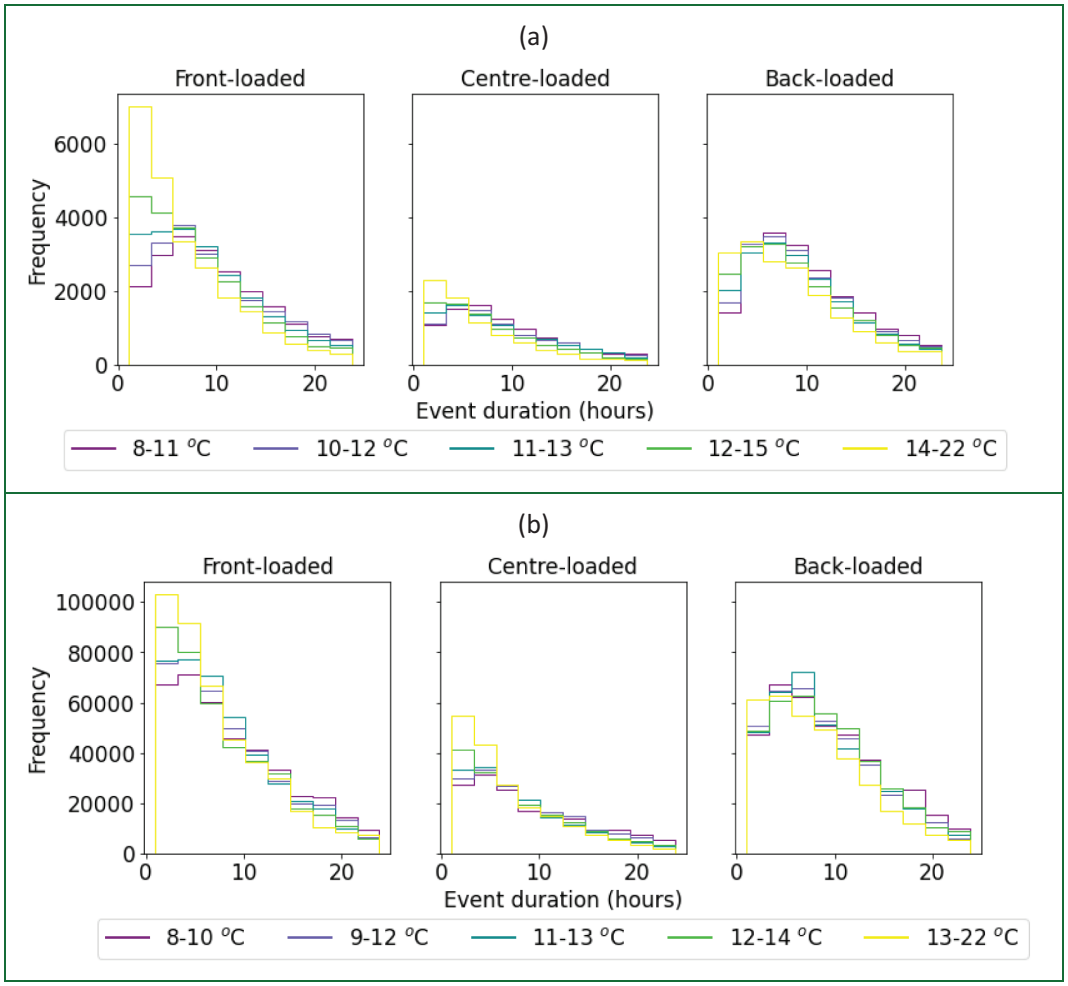

FIGURE 3 | Event duration frequency for observed (panel (a)) and CONVEX CPM present-day (panel (b)) profiles with dewpoint temperature using five equal-number temperature bins. Histogram colours indicate their temperature bins from cool (purple) to warm (yellow), illustrating that warmer temperature conditions are associated with a higher frequency of short-duration events. [Colour figure can be viewed at wileyonlinelibrary.com]

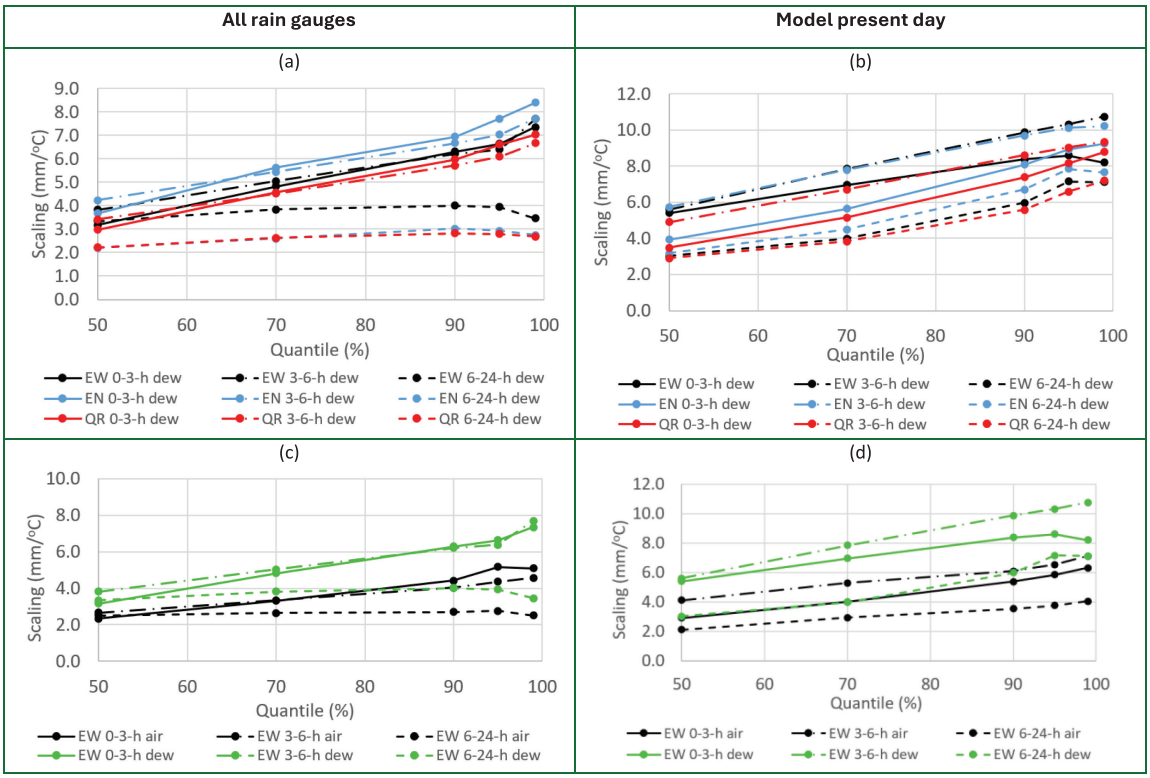

FIGURE 4 | Rainfall depth scaling slopes for events of < 3 h, 3–6 h and 6–24 h duration. The upper-left panel (a) compares observational scaling with dewpoint temperature results using equal-width (EW) binning (black), equal-number (EN) binning (blue) and quantile regression (QR) (red). The lower-left panel (c) compares observational results for scaling with air temperature (black) and dewpoint temperature (green). The right-hand panels (b) and (d) show corresponding results for the CONVEX CPM present-day simulation. [Colour figure can be viewed at wileyonlinelibrary.com]

scaling (Figure 4, all panels). Reduced scaling for longer duration events has been widely reported (Haerter et al. 2010; Hardwick Jones et al. 2010; Panthou et al. 2014) and may reflect their smaller convective component as several studies have found lower scaling for stratiform compared with convective rainfall (Berg et al. 2013; Molnar et al. 2015; Park and Min 2017), though the difference is minimal for the UK (Blenkinsop et al. 2015). However, other studies argue that apparent high scaling rates result not from physical differences but from the statistical mixing of rainfall types as conditions shift from predominantly stratiform to convective with increasing temperatures (Haerter and Berg 2009; Da Silva and Haerter 2025).

Results in Section 3.2 focus on events of < 3 h, which are most strongly convective. Scaling is shown for 3-h pre-event dewpoint temperature, although similar rates were obtained using 1-h pre-event dewpoint temperature (not shown) and air temperature (see Supporting Information Section S3).

3.2 | Scaling of Rainfall Event Characteristics With Dewpoint Temperature

Results are presented for observations using the all-raingauges (nationwide) pooling, and for the CPM domain (southern England and Wales) under present-day and future climates, showing scaling of rainfall event characteristics with dewpoint temperature.

Figure 5 panels (a), (c) and (e) show scaling of total event depth with dewpoint temperature. Observations exhibit sub-CC scaling at the median and approximately CC scaling at higher quantiles. The CPM shows similar behaviour for both time-slices, although present-day scaling is slightly higher. The observations do not cover as wide a range of rainfall depths as the CPM and samples are sparse in the upper depth range, hence the highest observational quantiles may be underestimated due to limited sample size. In contrast, the CPM future simulation shows a downturn in scaling at ~19°C consistent with the peak-like behaviour reported by Chan et al. (2015) for 1-h rainfall. While downturns in air temperature scaling are typically linked to moisture limitations (Prein et al. 2016), the use of dewpoint temperature suggests that other factors, such as mesoscale circulation, vertical instability or wind shear, may constrain rainfall at high temperatures (Lenderink et al. 2011; Blenkinsop et al. 2015).

Figure 5 panels (b), (d) and (f) present results for maximum event intensity, defined as the highest sub-hourly rainfall within an event. Rain gauges use 15-min data, while CPM outputs are at 10-min resolution; although this could allow higher rain gauge intensities in theory, the smaller observational sample limits the upper range. Scaling patterns are similar to those for event depth but with consistently higher rates, particularly in the CPM present-day simulation, where upper quantiles show clear super-CC behaviour. These findings indicate that warming exerts a stronger influence on maximum rainfall intensity than on total event depth.

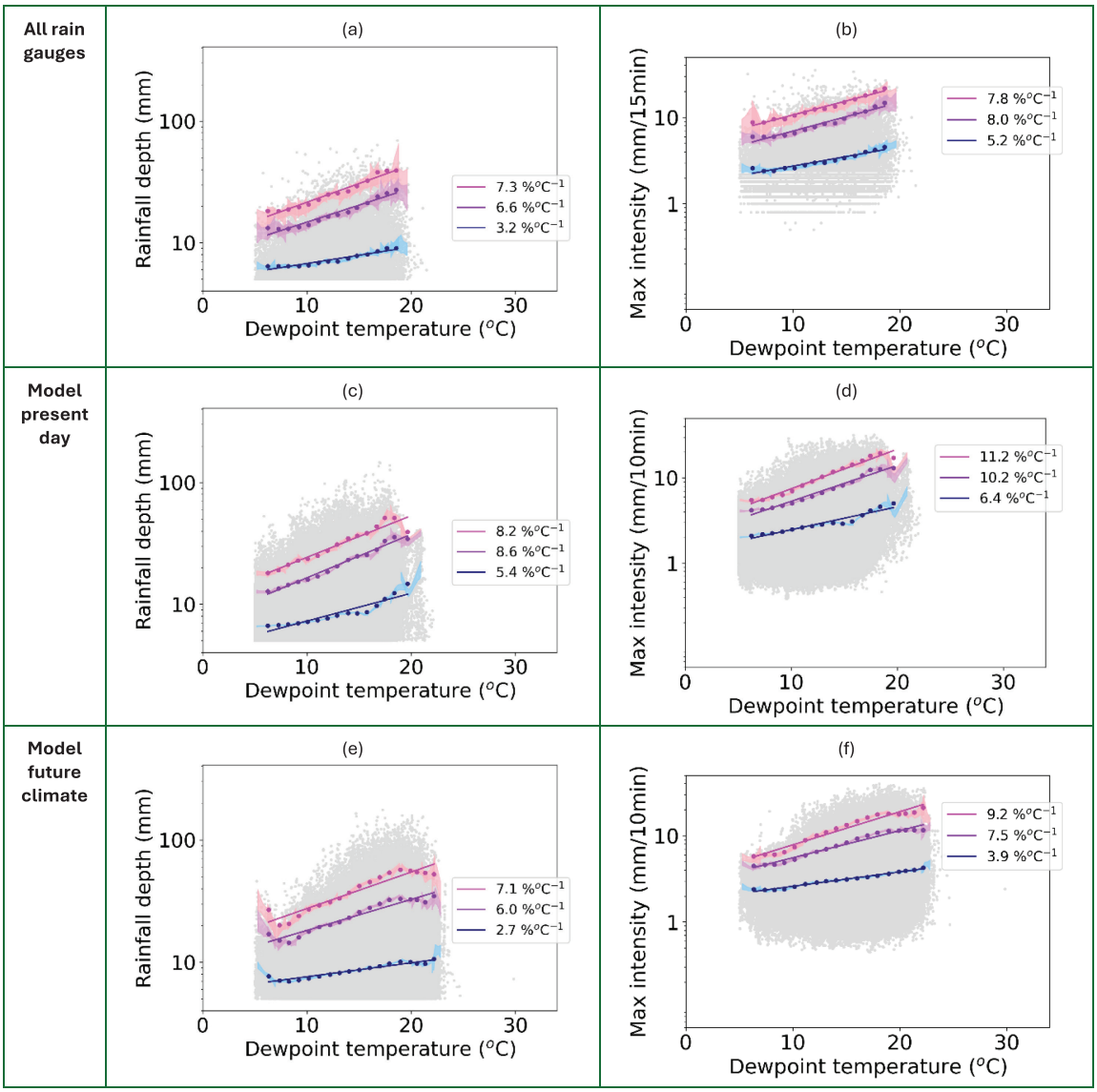

FIGURE 5 | Scaling of rainfall event total depth (panels (a), (c), (e)) and maximum intensity (panels (b), (d), (f)) with 3-h pre-event dewpoint temperature for observations and CONVEX CPM present-day and future climates. Individual rainfall events are shown as grey points. Coloured markers denote fitted 50th, 95th and 99th quantiles for each equal-width temperature bin, with corresponding regression lines shown in matching colours. 95% uncertainty ranges between the 2.75 and 97.5 percentiles have been calculated using bootstrapping and lowess fitting, and are shown as paler shading of each quantile's colour. [Colour figure can be viewed at wileyonlinelibrary.com]

An indication of uncertainty is shown using bootstrapping to calculate 95% confidence intervals for the quantile points. The bootstrapping took 1000 samples with replacement from each temperature bin and fitted a Lowess line to their 2.5 and 97.5 percentiles. The interval between each pair of Lowess lines is shaded in Figure 5. The results show greater uncertainty for the gauge events than for the model events, especially at higher quantiles and higher temperatures. This is most likely due to having fewer events, but it is interesting that there is a hint of a peak at about 19°C, followed by a reduction in gradient of the uncertainty range that is not so readily apparent from just the quantile points, which potentially suggests some support for the peak structure seen in the model scaling.

Scaling of rainfall event profile concentration with temperature was assessed using the PW_{50} metric (Table 1) with results shown in Figure 6 panels (a), (c) and (e). Negative scaling of PW_{50} with dewpoint temperature indicates that 50% of rainfall occurs over a shorter proportion of the event at higher temperatures, implying more temporally concentrated storms. This pattern aligns with the increase in maximum intensity under warming, though PW_{50} reflects behaviour across a longer fraction of the event duration. Scaling in the CPM present-day and future climates is slightly weaker than in observations; likely reflecting model limitations in fully resolving convective processes.

Scaling of rainfall event profile loading with temperature was assessed using the D_{50} metric (Table 1), with results shown in Figure 6 panels (b), (d) and (f). For observations, negative scaling of D_{50} with dewpoint temperature shows that 50% of event total depth occurs earlier at higher temperatures, indicating increasingly front-loaded events. The effect is stronger for lower quantiles; this suggests that already front-loaded events become notably more so with warming, while back-loaded events loading

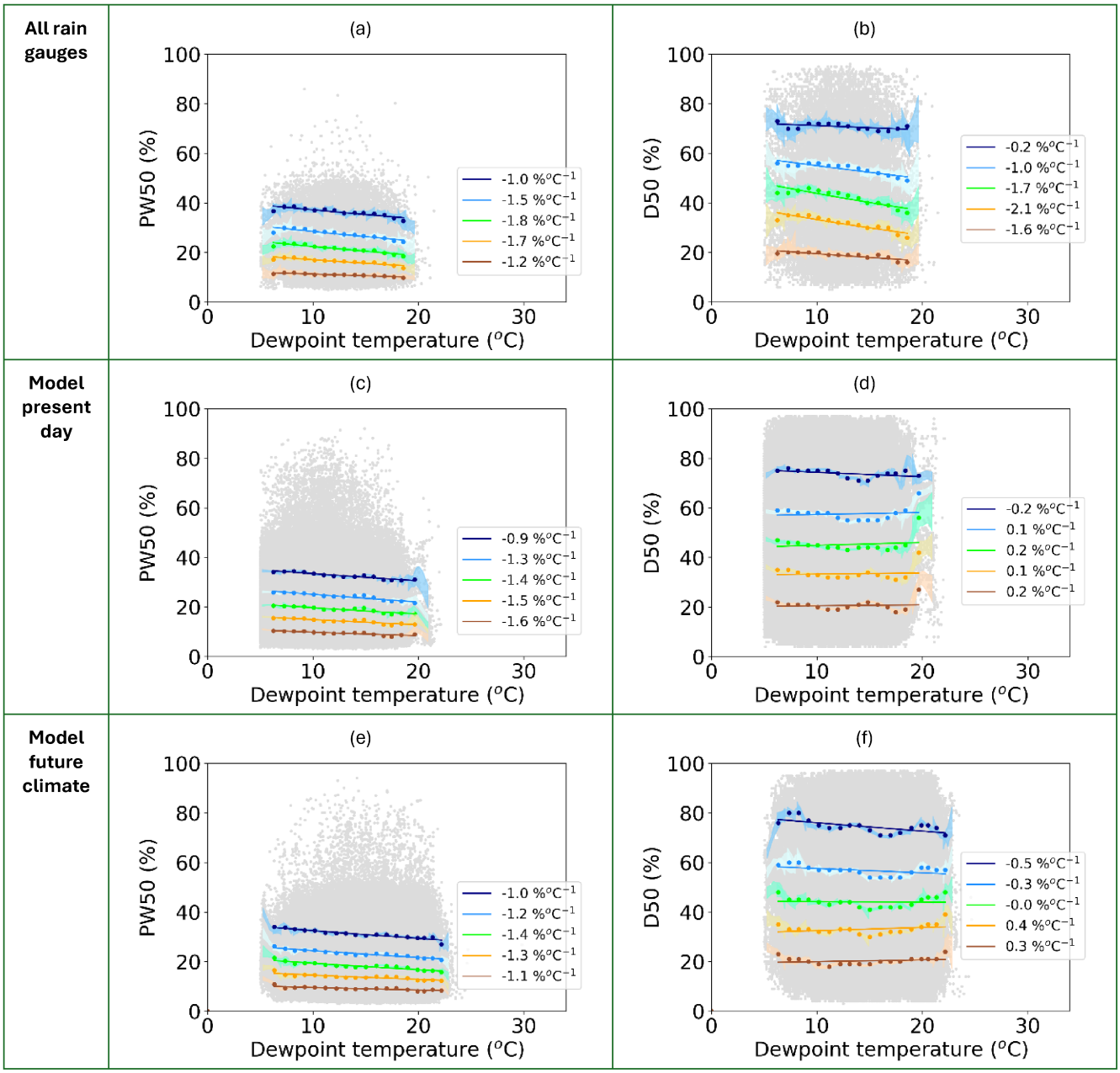

FIGURE 6 | Scaling of rainfall event PW_{50} (panels (a), (c), (e)) and D_{50} (panels (b), (d), (f)) with 3-h pre-event dewpoint temperature for observations and CONVEX CPM present-day and future climates. Individual rainfall events are shown as grey points. Coloured markers denote fitted quantiles from 10% to 90% at 20% intervals for each equal-width temperature bin, with corresponding regression lines shown in matching colours. 95% uncertainty ranges between the 2.75 and 97.5 percentiles have been calculated using bootstrapping and lowess fitting, and are shown as paler shading of each quantile's colour. [Colour figure can be viewed at wileyonlinelibrary.com]

shifts earlier but the change is smaller. The CPM reproduces this general pattern for < 3 h back-loaded events, though with slightly weaker slopes. However, CPM < 3 h front-loaded events show weak positive scaling, inconsistent with observations. This inconsistency is only seen for < 3 h events—for longer-duration CPM events D_{50} shows negative scaling, which are likewise more strongly negative for lower D_{50} (e.g., CPM 3–6 h scaling (not shown) of −1.2, −1.9, −1.6, −1.2 and −0.8%°C^{-1} for q10 to q90, respectively). The discrepancy at shorter durations suggest the CPM may not initiate intense rainfall rapidly enough at event onset, resulting in higher D_{50} values and a systematic bias that warrants further investigation.

The 95% uncertainty ranges from bootstrapping are indicated by the shaded intervals in Figure 6. Again, the uncertainty is greater at higher quantiles and higher temperatures, especially for D_{50}. Usually, the gauge data has wider uncertainty ranges than the model; however, it is noted that the model present day (Figure 6 panel (d)) shows some spurious values at the highest temperatures due to the available samples. Whilst the trend of the scaling is visually clear (e.g., clear downwards trends overall can be seen for both PW_{50} and D_{50}), the uncertainty ranges highlight the difficulty of relying on summary regression slope values, which can be affected by sample numbers in the different temperature bins, especially the first and

last. This may partly explain the lack of a clear pattern in the regression slope gradients at different quantiles when the regression slope absolute values are very small (e.g., see Figure 6 panel (d), where slope values increase and decrease from the 10th to 90th quantile).

The relationship between rainfall profile shape and temperature is illustrated in Figure 7 using normalised cumulative rainfall plots. All < 3 h events were grouped into 2°C dewpoint bins, and the median profile for each bin was plotted. Colder events (purple) show a slower rise in cumulative rainfall, reaching D_{50} later and indicating more back-loaded profiles. In contrast, warmer events (green to yellow) rise more rapidly, reaching D_{50} earlier and indicating increasingly front-loaded profiles. Differences in PW_{50} with temperature are subtler: colder events display more uniform, near-straight line profiles, indicating less concentrated rainfall, while warmer events exhibit greater curvature in the event profile, where rainfall is concentrated. These temperature-dependent changes are more pronounced in observations than in the model simulations; the modelled profiles are more uniform, suggesting the CPM underrepresents the observed warming-related shift in profile shape.

4 | Discussion

Current UK flood estimation guidance accounts for climate change through uniform uplift factors applied to rainfall or flow (Llywodraeth Cymru/Welsh Government 2021; Ministry of Housing et al. 2023; Scottish Environment Protection Agency/Buidheann Dion. Àrainneachd na h-Alba 2024), but does not yet consider how the temporal structure of rainfall events may change. This study analyses the scaling of rainfall profile metrics with dewpoint temperature to assess how event intensity and timing may evolve within the warmer climate projected for both dry bulb and dewpoint temperature (Kendon, Fosser, et al. 2019). Results show that storm profiles vary systematically with temperature.

Scaling of rainfall event total depth (≈6–8%°C^{-1}) and maximum intensity (≈7–11%°C^{-1}) show both increase with dewpoint temperature, with stronger scaling for maximum intensity, indicating that future storms will produce greater volumes and sharper peaks. Scaling rates are highest for extreme quantiles, suggesting that the most severe events will intensify most strongly—consistent with previous findings (Lenderink and Van Meijgaard 2010; Panthou et al. 2014; Molnar et al. 2015; Ali, Fowler, et al. 2021; Ali, Peleg, and Fowler 2021). Other studies considering maximum intensity within a temporal profile are few, but a study of Australian rain gauge data (Wasko and Sharma 2015) similarly found maximum intensity increased with dewpoint and dry bulb air temperature, while a study of a sample of rain gauges in north-west England (Fadhel et al. 2018) also found maximum intensity increased with dry bulb air temperature (dewpoint was not analysed). PW_{50} scaling shows that at higher temperatures, 50% of event rainfall occurs within a shorter proportion of the storm duration, suggesting that storm rainfall will become more concentrated in a warmer future. This is consistent with the increase in maximum intensity, although scaling magnitudes are smaller (≈1–2%°C^{-1}) for PW_{50} than for maximum intensity (≈4–11%°C^{-1}). This indicates that future storms will not only have sharper peaks, but the majority of the rainfall will be compressed into a shorter timeframe, producing highly intense rainfall bursts within the storm. Furthermore, D_{50} scaling shows that events also become increasingly front-loaded at warmer temperatures, though changes in event timing (≈1–2%°C^{-1}) are weaker than changes in magnitude. Analysis of rain gauge data in Australia with dry bulb and dewpoint temperature (Visser et al. 2023) similarly indicated a decrease in D_{50}. The changes in event timing are clearer in observations than in the CPM, likely reflecting model limitations in simulating early convective initiation. It is noted that the scaling values obtained here are dependent on the regions and events analysed. Event mixing effects and sample-size constraints remain challenges for scaling studies, as pooling data across space and duration can dilute local

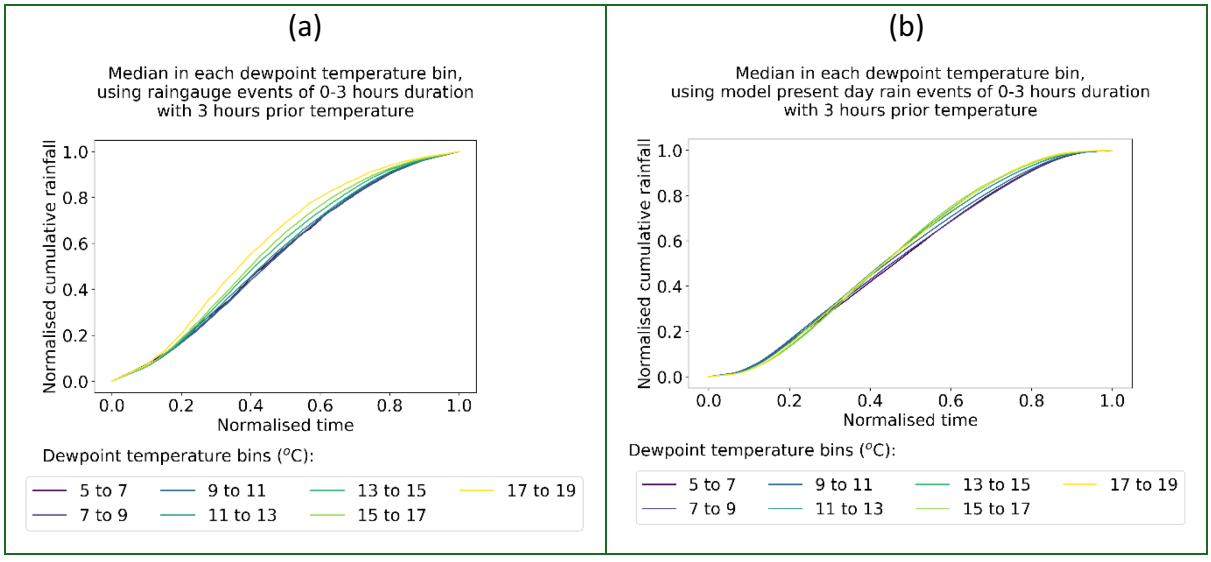

FIGURE 7 | Normalised cumulative median profiles over a range of 2°C temperature bins, for observations (panel (a)) and CPM present-day (panel (b)) for 3-h pre-event dewpoint temperature. [Colour figure can be viewed at wileyonlinelibrary.com]

effects (e.g., see Supporting Information Section S3 for results using further regional subdivision).

The CPM reproduces observed scaling patterns reasonably well for rainfall depth, maximum intensity and concentration, providing some confidence in its projections. It shows similar scaling to observations for D_{50} in longer-duration events, although it cannot reproduce observed D_{50} scaling for short-duration, front-loaded events at high temperatures. The CPM future simulations show weaker scaling than present-day, suggesting that rainfall-temperature relationships may not scale linearly under long-term warming. This may reflect physical limits imposed by atmospheric moisture and stability, or internal constraints within the model system.

The projected increases in rainfall depth, intensity and concentration imply a higher flash flood potential (Doswell et al. 1996). Larger rainfall volumes delivered in a shorter timeframe could increase flood depth, velocity and hazard, particularly in urban and rapid-response catchments (Dale 2021). Conversely, the greater front-loading of storms has contrasting implications: the shorter time to peak intensity reduces flood warning lead times thus increasing flood risk; however, several previous studies have indicated that front-loaded rainfall profiles generally lead to lower hydrograph peaks than back-loaded profiles thus reducing flood risk (Dullo et al. 2017; Chen et al. 2018; Hettiarachchi et al. 2018; Cheng et al. 2020; Mei et al. 2020; Yuan et al. 2022). If rainfall is front-loaded then much of the peak rainfall is lost to soil infiltration, depression filling and vegetation interception, whereas for backloaded rainfall, by the time the peak rainfall occurs these storages have already been filled, thus higher runoff rates can occur (Hettiarachchi et al. 2018; Yuan et al. 2022). Other factors will also modulate flood risk. Warmer temperatures will increase soil moisture evaporation leading to drier catchments, potentially lowering flood risk in rural catchments, although not in urban areas with limited storage; however, large rainfall events can still overwhelm soil infiltration capacity (Wasko et al. 2021), with this risk increasing for future events with greater volume and intensity. Given that flash-flooding already presents significant danger to life (Jonkman 2005; Doocy et al. 2013; Hu et al. 2018; Archer and Fowler 2021; Dale 2021), further work on understanding how rainfall dynamics interact with antecedent conditions is crucial.

Beyond flooding, changes in rainfall profile shape have broader implications. More intense bursts can increase soil erosion (Wang et al. 2022). 'First-flush' pollution, which relates to the pollutant load transported in the initial runoff volume from urban surfaces (Gao et al. 2023), may cause more severe effects if more intense and front-loaded storms cause rapid mobilisation even earlier in the storm, while receiving river levels are relatively low, although this may be mitigated by future increased storm depth offering more dilution potential. Greater rainfall depths, intensities and concentrations may more frequently overwhelm urban drainage systems and cause more sewer overflows without additional adaptation.

The limitations of this investigation include constraints on the thresholds, parameters and variables used to select the rainfall events and corresponding temperatures. Whilst some sensitivity testing has been undertaken, there are still numerous variations that could be explored in future studies. For example, a universal interarrival period of 7.5 h was applied to all gauges and the model, as in Hundhausen et al. (2025), with this threshold considered reasonable as it is approximately the mid-point of the range of interarrival periods determined for the quality-controlled rainfall dataset in Villalobos Herrera et al. (2023). However, it would be useful for further work to be undertaken considering other interarrival periods; in particular, shorter times would be likely to introduce additional events as a single convective storm cell will usually pass over a rain gauge in less than an hour, assuming some advection, so multiple cells may have come and gone within the interarrival period. However, the advantage of additional events needs to be balanced against the difficulty of ensuring independent events. The ERA-5-Land 0.25° resolution grid is relatively coarse for some areas, such as close to the coast, mountains or urban areas. Work is continually ongoing to improve reanalysis datasets; therefore, future work may be able to undertake this analysis with more locally nuanced dewpoint temperature variables. This will aid the comparison with the CPM which, having a finer grid resolution, better represents coastal, mountain and urban effects.

Overall, these findings emphasise that future storm hazards cannot be represented solely by uniform uplift factors on rainfall totals. Changes in rainfall temporal structure—particularly increased intensity, concentration and front-loading—should be explicitly integrated into design storm guidance and flood modelling to ensure effective adaption to a warming climate. It is emphasised that this study only considers summer, convective rainfall and further research would be required to assess changes in winter rainfall profiles.

5 | Conclusions

This study demonstrates that the temporal profiles of short-duration (< 3 h) rainfall events respond systematically to temperature, with warmer conditions producing storms of greater depth, maximum intensity, concentration and front-loading. However, this increase may not increase indefinitely; weaker scaling gradients in the future CPM simulations suggest possible physical or model-imposed limits. Physically, storm intensification has natural constraints—such as limits to how concentrated a rainfall event can become, while model limitations may also contribute, particularly the CPM's reduced ability to capture rapid convective initiation, as indicated by the D_{50} results.

These findings have clear implications for flood risk assessment. Current UK practice typically applies climate change uplift factors to rainfall totals without accounting for changes in temporal structure. Our results indicate that future design storms should reflect not only higher total depths, but also more intense, concentrated, and front-loaded profiles. Ignoring these temporal changes could underestimate flood hazards and misrepresent climate change impacts in hydrological modelling and infrastructure planning.

Author Contributions

Marie Hundhausen: software. **Stephen Blenkinsop:** writing – review and editing, supervision. **Alexandra Seawell:** funding acquisition, writing – original draft, methodology, visualization, writing – review and editing, software, formal analysis. **Hayley J. Fowler:** conceptualization, writing – review and editing, funding acquisition, supervision. **Roberto Villalobos Herrera:** software, data curation, supervision. **Haider Ali:** software, writing – review and editing. **Caspar J. M. Hewett:** writing – review and editing, supervision.

Acknowledgements

The authors would like to thank Elizabeth Kendon (UK Met Office), Abdullah Kahraman (Newcastle University), Colin Manning (Newcastle University), and Steven Chan (National Oceanography Centre (NOC)) for their help with supplying the CONVEX CPM outputs and answering queries.

Funding

Funding for the PhD to undertake this study was granted by the Engineering and Physical Science Research Council (EPSRC). H.J. Fowler was supported by the Co-Centre for Climate + Biodiversity + Water funded by UKRI (NE/Y006496/1) and a Royal Society Faraday Discovery Fellowship (FDF\S2\251,059).

Conflicts of Interest

The authors declare no conflicts of interest.

Data Availability Statement

The observed events analysis has been generated using Copernicus Atmosphere Monitoring Service Information 2024, specifically the ERA5-Land hourly data from 1950 to present 2 m air and dewpoint temperatures for Great Britain, available from Copernicus Climate Change Service (C3S) Climate Data Store (CDS) DOI: 10.24381/cds.e2161bac. Observed rainfall data is available from the Environment Agency, Scottish Environment Protection Agency and Natural Resources Wales, with quality-control scripts available at https://github.com/nclwater/SubHourlyQC. The simulated rainfall, 1.5 m air and dewpoint data have been obtained from the UK Met Office Convex climate model outputs of rainfall, air temperature and specific humidity.

References

Ali, H., H. J. Fowler, G. Lenderink, E. Lewis, and D. Pritchard. 2021. "Consistent Large-Scale Response of Hourly Extreme Precipitation to Temperature Variation Over Land." *Geophysical Research Letters* 48, no. 4: e2020GL090317. https://doi.org/10.1029/2020GL090317.

Ali, H., H. J. Fowler, and V. Mishra. 2018. "Global Observational Evidence of Strong Linkage Between Dew Point Temperature and Precipitation Extremes." *Geophysical Research Letters* 45, no. 22: 12320–12330. https://doi.org/10.1029/2018GL080557.

Ali, H., H. J. Fowler, D. Pritchard, G. Lenderink, S. Blenkinsop, and E. Lewis. 2022. "Towards Quantifying the Uncertainty in Estimating Observed Scaling Rates." *Geophysical Research Letters* 49, no. 12: e2022GL099138. https://doi.org/10.1029/2022GL099138.

Ali, H., and V. Mishra. 2017. "Contrasting Response of Rainfall Extremes to Increase in Surface Air and Dewpoint Temperatures at Urban Locations in India." *Scientific Reports* 7, no. 1: 1–15. https://doi.org/10.1038/s41598-017-01306-1.

Ali, H., N. Peleg, and H. J. Fowler. 2021. "Global Scaling of Rainfall With Dewpoint Temperature Reveals Considerable Ocean-Land Difference." *Geophysical Research Letters* 48, no. 15. https://doi.org/10.1029/2021GL093798.

Allan, R. P., D. A. Lavers, and A. J. Champion. 2016. "Diagnosing Links Between Atmospheric Moisture and Extreme Daily Precipitation Over the UK." *International Journal of Climatology* 36, no. 9: 3191–3206. https://doi.org/10.1002/JOC.4547.

Allen, M. R., and W. J. Ingram. 2002. "Constraints on Future Changes in Climate and the Hydrologic Cycle." *Nature. Nature Publishing Group* 419, no. 6903: 224–232. https://doi.org/10.1038/nature01092.

Archer, D., and H. Fowler. 2021. "A Historical Flash Flood Chronology for Britain." *Journal of Flood Risk Management* 14, no. 3: e12721. https://doi.org/10.1111/JFR3.12721.

Ban, N., J. Schmidli, and C. Schär. 2015. "Heavy Precipitation in a Changing Climate: Does Short-Term Summer Precipitation Increase Faster?" *Geophysical Research Letters* 42, no. 4: 1165–1172. https://doi.org/10.1002/2014GL062588.

Barbero, R., S. Westra, G. Lenderink, and H. J. Fowler. 2018. "Temperature-Extreme Precipitation Scaling: A Two-Way Causality?" *International Journal of Climatology* 38: e1274–e1279. https://doi.org/10.1002/JOC.5370.

Berg, P., and J. O. Haerter. 2013. "Unexpected Increase in Precipitation Intensity With Temperature — A Result of Mixing of Precipitation Types?" *Atmospheric Research* 119: 56–61. https://doi.org/10.1016/J.ATMOSRES.2011.05.012.

Berg, P., C. Moseley, and J. O. Haerter. 2013. "Strong Increase in Convective Precipitation in Response to Higher Temperatures." *Nature Geoscience* 6, no. 3: 181–185. https://doi.org/10.1038/NGEO1731.

Blenkinsop, S., S. C. Chan, E. J. Kendon, N. M. Roberts, and H. J. Fowler. 2015. "Temperature Influences on Intense UK Hourly Precipitation and Dependency on Large-Scale Circulation." *Environmental Research Letters* 10, no. 5: 054021. https://doi.org/10.1088/1748-9326/10/5/054021.

Blenkinsop, S., and H. J. Fowler. 2014. "An Hourly and Multi-Hourly Extreme Precipitation Climatology for the UK and Long-Term Changes in Extremes. *Vulnerability, Uncertainty, and Risk: Quantification, Mitigation, and Management - Proceedings of the*." In *2nd Int. Conf. On Vulnerability and Risk Analysis and Management, ICVRAM 2014 and the 6th Int. Symposium on Uncertainty Modeling and Analysis, ISUMA 2014*, 1385–1394. American Society of Civil Engineers. https://doi.org/10.1061/9780784413609.139.

Blenkinsop, S., E. Lewis, S. C. Chan, and H. J. Fowler. 2017. "Quality-Control of an Hourly Rainfall Dataset and Climatology of Extremes for the UK." *International Journal of Climatology* 37, no. 2: 722–740. https://doi.org/10.1002/JOC.4735.

Bolton, D. 1980. "The Computation of Equivalent Potential Temperature." *Monthly Weather Review* 108, no. 7: 1046–1053.

Cai, J. 2019. "Humidity Measures Webpage." https://cran.r-project.org/web/packages/humidity/vignettes/humidity-measures.html.

Chan, S. C., E. J. Kendon, H. J. Fowler, S. Blenkinsop, N. M. Roberts, and C. A. T. Ferro. 2014. "The Value of High-Resolution Met Office Regional Climate Models in the Simulation of Multihourly Precipitation Extremes." *Journal of Climate* 27, no. 16: 6155–6174. https://doi.org/10.1175/JCLI-D-13-00723.1.

Chan, S. C., E. J. Kendon, N. M. Roberts, H. J. Fowler, and S. Blenkinsop. 2015. "Downturn in Scaling of UK Extreme Rainfall With Temperature for Future Hottest Days." *Nature Geoscience* 9, no. 1: 24–28. https://doi.org/10.1038/NGEO2596.

Chan, S. C., E. J. Kendon, N. M. Roberts, H. J. Fowler, and S. Blenkinsop. 2016. "The Characteristics of Summer Sub-Hourly Rainfall Over the Southern UK in a High-Resolution Convective Permitting Model." *Environmental Research Letters* 11, no. 9: 094024. https://doi.org/10.1088/1748-9326/11/9/094024.

Chen, W., G. Huang, H. Zhang, and W. Wang. 2018. "Urban Inundation Response to Rainstorm Patterns With a Coupled Hydrodynamic Model: A Case Study in Haidian IslandChina." *Journal of Hydrology* 564: 1022–1035. https://doi.org/10.1016/J.JHYDROL.2018.07.069.

Chen, Z., L. Yin, X. Chen, S. Wei, and Z. Zhu. 2015. "Research on the Characteristics of Urban Rainstorm Pattern in the Humid Area of Southern China: A Case Study of Guangzhou City." *International Journal of Climatology* 35, no. 14: 4370–4386. https://doi.org/10.1002/JOC.4294.

Cheng, T., Z. Xu, H. Yang, S. Hong, and J. P. Leitao. 2020. "Analysis of Effect of Rainfall Patterns on Urban Flood Process by Coupled Hydrological and Hydrodynamic Modeling." *Journal of Hydrologic Engineering* 25, no. 1: 04019061. https://doi.org/10.1061/(ASCE)HE.1943-5584.0001867/ASSET/9F0C5142-B389-4E32-9E30-DCAFE47BD3EC/ASSETS/IMAGES/LARGE/FIGURE11.JPG.

Copernicus Climate Change Service (C3S). 2019. "ERA5-Land Hourly Data From 1950 to Present." Copernicus Climate Change Service (C3S) Climate Data Store (CDS). Accessed November 17, 2024. https://doi.org/10.24381/cds.e2161bac.

Da Silva, N. A., and J. O. Haerter. 2025. "Super-Clausius–Clapeyron Scaling of Extreme Precipitation Explained by Shift From Stratiform to Convective Rain Type." *Nature Geoscience* 18, no. 5: 382–388. https://doi.org/10.1038/S41561-025-01686-4;SUBJMETA=106,2786,35,694,704,823;KWRD=ATMOSPHERIC+DYNAMICS,CLIMATE+CHANGE,PROJECTION+AND+PREDICTION.

Dale, M. 2021. "Managing the Effects of Extreme Sub-Daily Rainfall and Flash Floods - a Practitioner's Perspective." *Philosophical Transactions of the Royal Society A* 379, no. 2195: 20190550. https://doi.org/10.1098/RSTA.2019.0550.

Darwish, M. M., H. J. Fowler, S. Blenkinsop, and M. R. Tye. 2018. "A Regional Frequency Analysis of UK Sub-Daily Extreme Precipitation and Assessment of Their Seasonality." *International Journal of Climatology* 38, no. 13: 4758–4776. https://doi.org/10.1002/JOC.5694.

Darwish, M. M., M. R. Tye, A. F. Prein, et al. 2021. "New Hourly Extreme Precipitation Regions and Regional Annual Probability Estimates for the UK." *International Journal of Climatology* 41, no. 1: 582–600. https://doi.org/10.1002/JOC.6639.

Doocy, S., A. Daniels, S. Murray, and T. D. Kirsch. 2013. "The Human Impact of Floods: A Historical Review of Events 1980-2009 and Systematic Literature Review." *PLoS Currents* 5. https://doi.org/10.1371/CURRENTS.DIS.F4DEB457904936B07C09DAA98EE8171A.

Doswell, C. A., H. E. Brooks, and R. A. Maddox. 1996. "Flash Flood Forecasting: An Ingredients-Based Methodology." *Weather and Forecasting* 11, no. 4: 560–581. https://doi.org/10.1175/1520-0434(1996)011<0560:FFFAIB>2.0.CO;2.

Dullo, T. T., A. J. Kalyanapu, and R. S. V. Teegavarapu. 2017. "Evaluation of Changing Characteristics of Temporal Rainfall Distribution Within 24-Hour Duration Storms and Their Influences on Peak Discharges: Case Study of Asheville, North Carolina." *Journal of Hydrologic Engineering* 22, no. 11: 05017022. https://doi.org/10.1061/(ASCE)HE.1943-5584.0001575/ASSET/1F4A1512-0ADA-453F-BE68-F3B79BF0C01C/ASSETS/IMAGES/LARGE/FIGURE13.JPG.

Fadhel, S., M. A. Rico-Ramirez, and D. Han. 2018. "Sensitivity of Peak Flow to the Change of Rainfall Temporal Pattern due to Warmer Climate." *Journal of Hydrology* 560: 546–559. https://doi.org/10.1016/J.JHYDROL.2018.03.041.

Fowler, H. J., H. Ali, R. P. Allan, et al. 2021. "Towards Advancing Scientific Knowledge of Climate Change Impacts on Short-Duration Rainfall Extremes." *Philosophical Transactions of the Royal Society A* 379, no. 2195: 20190542. https://doi.org/10.1098/RSTA.2019.0542.

Gao, Z., Q. Zhang, J. Li, Y. Wang, M. Dzakpasu, and X. C. Wang. 2023. "First Flush Stormwater Pollution in Urban Catchments: A Review of Its Characterization and Quantification Towards Optimization of Control Measures." *Journal of Environmental Management* 340: 117976. https://doi.org/10.1016/j.jenvman.2023.117976.

Ghanghas, A., A. Sharma, and V. Merwade. 2024. "Unveiling the Evolution of Extreme Rainfall Storm Structure Across Space and Time in a Warming Climate." *Earth's Future* 12, no. 9: e2024EF004675. https://doi.org/10.1029/2024EF004675.

Haerter, J. O., and P. Berg. 2009. "Unexpected Rise in Extreme Precipitation Caused by a Shift in Rain Type?" *Nature Geoscience* 2, no. 6: 372–373. https://doi.org/10.1038/NGEO523.

Haerter, J. O., P. Berg, and S. Hagemann. 2010. "Heavy Rain Intensity Distributions on Varying Time Scales and at Different Temperatures." *Journal of Geophysical Research: Atmospheres* 115, no. D17: 17102. https://doi.org/10.1029/2009JD013384.

Hand, W. H., N. I. Fox, and C. G. Collier. 2004. "A Study of Twentieth-Century Extreme Rainfall Events in the United Kingdom With Implications for Forecasting." *Meteorological Applications* 11, no. 1: 15–31. https://doi.org/10.1017/S1350482703001117.

Hardwick Jones, R., S. Westra, and A. Sharma. 2010. "Observed Relationships Between Extreme Sub-Daily Precipitation, Surface Temperature, and Relative Humidity." *Geophysical Research Letters* 37, no. 22. https://doi.org/10.1029/2010GL045081.

Hettiarachchi, S., C. Wasko, and A. Sharma. 2018. "Increase in Flood Risk Resulting From Climate Change in a Developed Urban Watershed - The Role of Storm Temporal Patterns." *Hydrology and Earth System Sciences* 22, no. 3: 2041–2056. https://doi.org/10.5194/HESS-22-2041-2018.

Hu, P., Q. Zhang, P. Shi, B. Chen, and J. Fang. 2018. "Flood-Induced Mortality Across the Globe: Spatiotemporal Pattern and Influencing Factors." *Science of the Total Environment* 643: 171–182. https://doi.org/10.1016/J.SCITOTENV.2018.06.197.

Hundhausen, M., H. Feldmann, R. Kohlhepp, and J. G. Pinto. 2024. "Climate Change Signals of Extreme Precipitation Return Levels for Germany in a Transient Convection-Permitting Simulation Ensemble." *International Journal of Climatology* 44, no. 5: 1454–1471. https://doi.org/10.1002/JOC.8393;PAGE:STRING:ARTICLE/CHAPTER.

Hundhausen, M., H. J. Fowler, H. Feldmann, and J. G. Pinto. 2025. "Sub-Hourly Precipitation and Rainstorm Event Profiles in a Convection-Permitting Multi-GCM Ensemble." *Weather and Climate Extremes* 48: 100764. https://doi.org/10.1016/J.WACE.2025.100764.

Intergovernmental Panel on Climate Change. 2021. *Climate Change 2021: The Physical Science Basis. Contribution of Working Group I to the Sixth Assessment Report of the Intergovernmental Panel on Climate Change*. Edited by V. Masson-Delmotte, P. Zhai, A. Pirani, et al. Cambridge University Press.

Jones, M. R., S. Blenkinsop, H. J. Fowler, and C. G. Kilsby. 2014. "Objective Classification of Extreme Rainfall Regions for the UK and Updated Estimates of Trends in Regional Extreme Rainfall." *International Journal of Climatology* 34, no. 3: 751–765. https://doi.org/10.1002/JOC.3720.

Jonkman, S. N. 2005. "Global Perspectives on Loss of Human Life Caused by Floods." *Natural Hazards* 34, no. 2: 151–175. https://doi.org/10.1007/S11069-004-8891-3.

Kendon, E., G. Fosser, J. Murphy, et al. 2019. *UKCP Convection-Permitting Model Projections: Science Report*. Met Office.

Kendon, E. J., N. M. Roberts, H. J. Fowler, M. J. Roberts, S. C. Chan, and C. A. Senior. 2014. "Heavier Summer Downpours With Climate Change Revealed by Weather Forecast Resolution Model." *Nature Climate Change* 4, no. 7: 570–576. https://doi.org/10.1038/NCLIMATE2258.

Kendon, E. J., N. M. Roberts, C. A. Senior, and M. J. Roberts. 2012. "Realism of Rainfall in a Very High-Resolution Regional Climate Model." *Journal of Climate* 25, no. 17: 5791–5806. https://doi.org/10.1175/JCLI-D-11-00562.1.

Kendon, E. J., C. Short, J. Pope, et al. 2021. "Update to UKCP Local (2.2 km) Projections."

Kendon, E. J., R. A. Stratton, S. Tucker, et al. 2019. "Enhanced Future Changes in Wet and Dry Extremes Over Africa at Convection-Permitting Scale." *Nature Communications* 10, no. 1: 1–14. https://doi.org/10.1038/s41467-019-09776-9.

Lana, X., R. Rodríguez-Solà, M. D. Martínez, M. C. Casas-Castillo, C. Serra, and A. Burgueño. 2020. "Characterization of Standardized Heavy Rainfall Profiles for Barcelona City: Clustering, Rain Amounts and Intensity Peaks." *Theoretical and Applied Climatology* 142, no. 1–2: 255–268. https://doi.org/10.1007/S00704-020-03315-Z/TABLES/5.

Lawrence, M. G. 2005. "The Relationship Between Relative Humidity and the Dewpoint Temperature in Moist Air: A Simple Conversion and Applications." *Bulletin of the American Meteorological Society. American Meteorological Society* 86, no. 2: 225–234. https://doi.org/10.1175/BAMS-86-2-225.

Lenderink, G., H. Y. Mok, T. C. Lee, and G. J. Van Oldenborgh. 2011. "Scaling and Trends of Hourly Precipitation Extremes in Two Different Climate Zones - Hong Kong and The Netherlands." *Hydrology and Earth System Sciences* 15, no. 9: 3033–3041. https://doi.org/10.5194/HESS-15-3033-2011.

Lenderink, G., and E. van Meijgaard. 2008. "Increase in Hourly Precipitation Extremes Beyond Expectations From Temperature Changes." *Nature Geoscience* 1, no. 8: 511–514. https://doi.org/10.1038/ngeo262.

Lenderink, G., and E. Van Meijgaard. 2010. "Linking Increases in Hourly Precipitation Extremes to Atmospheric Temperature and Moisture Changes." *Environmental Research Letters* 5: 25208–25217. https://doi.org/10.1088/1748-9326/5/2/025208.

Llywodraeth Cymru/Welsh Government. 2021. *Planning Policy Wales, Technical Advice Note (TAN) 15: Development, flooding and coastal erosion*.

Lowe, J. A., D. Bernie, P. Bett, et al. 2019. *UKCP18 Science Overview Report*. Met Office.

Magan, B., S. Kim, C. Wasko, et al. 2020. "Impact of Atmospheric Circulation on the Rainfall-Temperature Relationship in Australia." *Environmental Research Letters* 15, no. 9: 094098. https://doi.org/10.1088/1748-9326/ABAB35.

Mei, C., J. H. Liu, H. Wang, et al. 2020. "Urban Flood Inundation and Damage Assessment Based on Numerical Simulations of Design Rainstorms With Different Characteristics." *SCIENCE CHINA Technological Sciences* 63, no. 11: 2292–2304. https://doi.org/10.1007/S11431-019-1523-2/METRICS.

Met Office Hadley Centre. 2022. "UK Climate Projections: Headline Findings (UKCP18) v4.0."

Ministry of Housing, Communities and Local Government, Department for Levelling Up, Housing and Communities. 2023. *National Planning Policy Framework (NPPF)*.

Molnar, P., S. Fatichi, L. Gaál, J. Szolgay, and P. Burlando. 2015. "Storm Type Effects on Super Clausius-Clapeyron Scaling of Intense Rainstorm Properties With Air Temperature." *Hydrology and Earth System Sciences* 19, no. 4: 1753–1766. https://doi.org/10.5194/HESS-19-1753-2015.

Najibi, N., S. Mukhopadhyay, and S. Steinschneider. 2022. "Precipitation Scaling With Temperature in the Northeast US: Variations by Weather Regime, Season, and Precipitation Intensity." *Geophysical Research Letters* 49, no. 8: e2021GL097100. https://doi.org/10.1029/2021GL097100.

Pan, C., X. Wang, L. Liu, D. Wang, and H. Huang. 2019. "Characteristics of Heavy Storms and the Scaling Relation With Air Temperature by Event Process-Based Analysis in South China." *Water* 11, no. 2: 185. https://doi.org/10.3390/W11020185.

Panthou, G., A. Mailhot, E. Laurence, and G. Talbot. 2014. "Relationship Between Surface Temperature and Extreme Rainfalls: A Multi-Time-Scale and Event-Based Analysis." *Journal of Hydrometeorology* 15, no. 5: 1999–2011. https://doi.org/10.1175/JHM-D-14-0020.1.

Park, I. H., and S. K. Min. 2017. "Role of Convective Precipitation in the Relationship Between Subdaily Extreme Precipitation and Temperature." *Journal of Climate* 30, no. 23: 9527–9537. https://doi.org/10.1175/JCLI-D-17-0075.1.

Pedregosa, F., G. Varoquaux, A. Gramfort, et al. 2011. "Scikit-Learn: Machine Learning in Python." *Journal of Machine Learning Research* 12, no. 85: 2825–2830.

Peleg, N., F. Marra, S. Fatichi, et al. 2018. "Intensification of Convective Rain Cells at Warmer Temperatures Observed From High-Resolution Weather Radar Data." *Journal of Hydrometeorology* 19, no. 4: 715–726. https://doi.org/10.1175/JHM-D-17-0158.1.

Prein, A. F., R. M. Rasmussen, K. Ikeda, C. Liu, M. P. Clark, and G. J. Holland. 2016. "The Future Intensification of Hourly Precipitation Extremes. *Nature Climate Change 2016 7:1*." *Nature Publishing Group* 7, no. 1: 48–52. https://doi.org/10.1038/NCLIMATE3168.

Pumo, D., G. Carlino, S. Blenkinsop, E. Arnone, H. Fowler, and L. V. Noto. 2019. "Sensitivity of Extreme Rainfall to Temperature in Semi-Arid Mediterranean Regions." *Atmospheric Research* 225: 30–44. https://doi.org/10.1016/J.ATMOSRES.2019.03.036.

Rico-Ramirez, M. A., S. Liguori, and A. N. A. Schellart. 2015. "Quantifying Radar-Rainfall Uncertainties in Urban Drainage Flow Modelling." *Journal of Hydrology* 528: 17–28. https://doi.org/10.1016/J.JHYDROL.2015.05.057.

Scottish Environment Protection Agency/Buidheann Dion. Àrainneachd na h-Alba. 2024. *Climate change allowances for flood risk assessment in land use planning: Version 5*.

Singleton, A., and R. Toumi. 2013. "Super-Clausius–Clapeyron Scaling of Rainfall in a Model Squall Line." *Quarterly Journal of the Royal Meteorological Society* 139, no. 671: 334–339. https://doi.org/10.1002/QJ.1919.

Skipper, S., and J. Perktold. 2010. "Statsmodels: Econometric and Statistical Modeling With Python. Proceedings of the 9th Python in Science Conference."

Stephens, G. L., T. L'Ecuyer, R. Forbes, et al. 2010. "Dreary State of Precipitation in Global Models." *Journal of Geophysical Research: Atmospheres* 115, no. D24: 24211. https://doi.org/10.1029/2010JD014532.

Trenberth, K. E. 1999. "Conceptual Framework for Changes of Extremes of the Hydrological Cycle With Climate Change." *Climatic Change* 42, no. 1: 327–339. https://doi.org/10.1023/A:1005488920935/METRICS.

Trenberth, K. E., A. Dai, R. M. Rasmussen, and D. B. Parsons. 2003. "The Changing Character of Precipitation." *Bulletin of the American Meteorological Society* 84, no. 9: 1205–1218. https://doi.org/10.1175/BAMS-84-9-1205.

Utsumi, N., S. Seto, S. Kanae, E. E. Maeda, and T. Oki. 2011. "Does Higher Surface Temperature Intensify Extreme Precipitation?" *Geophysical Research Letters* 38, no. 16: 16708. https://doi.org/10.1029/2011GL048426.

Van de Vyver, H., B. Van Schaeybroeck, R. De Troch, R. Hamdi, and P. Termonia. 2019. "Modeling the Scaling of Short-Duration Precipitation Extremes With Temperature." *Earth and Space Science* 6, no. 10: 2031–2041. https://doi.org/10.1029/2019EA000665.

Villalobos Herrera, R., S. Blenkinsop, S. B. Guerreiro, and H. J. Fowler. 2023. "The Creation and Climatology of a Large Independent Rainfall Event Database for Great Britain." *International Journal of Climatology* 43, no. 13: 6020–6037. https://doi.org/10.1002/JOC.8187.

Villalobos-Herrera, R., S. Blenkinsop, S. B. Guerreiro, T. O'Hara, and H. J. Fowler. 2022. "Sub-Hourly Resolution Quality Control of

Rain-Gauge Data Significantly Improves Regional Sub-Daily Return Level Estimates." *Quarterly Journal of the Royal Meteorological Society* 148, no. 748: 3252–3271. https://doi.org/10.1002/QJ.4357;SUBPAGE:STRING:FULL.

Visser, J. B., C. Wasko, A. Sharma, and R. Nathan. 2021. "Eliminating the "Hook" in Precipitation–Temperature Scaling." *Journal of Climate* 34, no. 23: 9535–9549. https://doi.org/10.1175/JCLI-D-21-0292.1.

Visser, J. B., C. Wasko, A. Sharma, and R. Nathan. 2023. "Changing Storm Temporal Patterns With Increasing Temperatures Across Australia." *Journal of Climate* 36, no. 18: 6247–6259. https://doi.org/10.1175/JCLI-D-22-0694.1.

Wang, G., D. Wang, K. E. Trenberth, et al. 2017. "The Peak Structure and Future Changes of the Relationships Between Extreme Precipitation and Temperature." *Nature Climate Change* 7, no. 4: 268–274. https://doi.org/10.1038/nclimate3239.

Wang, W., S. Yin, G. Gao, S. M. Papalexiou, and Z. Wang. 2022. "Increasing Trends in Rainfall Erosivity in the Yellow River Basin From 1971 to 2020." *Journal of Hydrology* 610: 127851. https://doi.org/10.1016/J.JHYDROL.2022.127851.

Wasko, C., R. Nathan, L. Stein, and D. O'Shea. 2021. "Evidence of Shorter More Extreme Rainfalls and Increased Flood Variability Under Climate Change." *Journal of Hydrology* 603: 126994. https://doi.org/10.1016/J.JHYDROL.2021.126994.

Wasko, C., and A. Sharma. 2014. "Quantile Regression for Investigating Scaling of Extreme Precipitation With Temperature." *Water Resources Research* 50, no. 4: 3608–3614. https://doi.org/10.1002/2013WR015194.

Wasko, C., and A. Sharma. 2015. "Steeper Temporal Distribution of Rain Intensity at Higher Temperatures Within Australian Storms." *Nature Geoscience* 8, no. 7: 527–529. https://doi.org/10.1038/NGEO2456.

Wilkinson, J. M., A. N. F. Porson, F. J. Bornemann, M. Weeks, P. R. Field, and A. P. Lock. 2013. "Improved Microphysical Parametrization of Drizzle and Fog for Operational Forecasting Using the Met Office Unified Model." *Quarterly Journal of the Royal Meteorological Society* 139, no. 671: 488–500. https://doi.org/10.1002/QJ.1975;JOURNAL:JOURNAL:1477870X;WGROUP:STRING:PUBLICATION.

Xie, Z., Y. Fu, H. S. He, S. Wang, L. Wang, and C. Liu. 2025. "Robust Assessment of Precipitation-Temperature Apparent Scaling Under Global Climate Change." *Journal of Hydrology* 656: 132957. https://doi.org/10.1016/J.JHYDROL.2025.132957.

Yuan, W., L. Lu, H. Song, et al. 2022. "Study on the Early Warning for Flash Flood Based on Random Rainfall Pattern." *Water Resources Management* 36, no. 5: 1587–1609. https://doi.org/10.1007/S11269-022-03106-3/FIGURES/10.

Supporting Information

Additional supporting information can be found online in the Supporting Information section. **Figure S1:** Three methods for scaling of rainfall profile D_{50} with 3-h pre-event air temperature for observations rainfall events of 0–3 h duration (upper panels) and 3–6 h duration (lower panels). Upper panels show typical results for equal-width bins (panel (a)), equal-number bins (panel (b)) and quantile regression (panel (c)). Lower panels illustrate key features, showing peaks and troughs for equal-width bins (panel (d)), smoother quantiles over smaller range for equal-number bins (panel (e)), and curvature of quantile regression due to limited sample range at low temperature (panel (f)). **Figure S2:** Scaling of rainfall event depth with 3-h pre-event air temperature for all-raingauges, regional rain gauges and CPM present-day and future climates. Rainfall events are shown as grey points, with fitted quantiles shown of 50%, 95% and 99% for each equal-width bin in coloured points and regression lines for each set of quantiles in correspondingly coloured lines. **Figure S3:** Scaling of rainfall event depth with 3-h pre-event dewpoint temperature for all-raingauges, regional rain gauges and CPM present-day and future climates. Rainfall events are shown as grey points, with fitted quantiles shown of 50%, 95% and 99% for each equal-width bin in coloured points and regression lines for each set of quantiles in correspondingly coloured lines. **Figure S4:** Scaling of rainfall event maximum intensity with 3-h pre-event air temperature for all-raingauges, regional rain gauges and CPM present-day and future climates. Rainfall events are shown as grey points, with fitted quantiles shown of 50%, 95% and 99% for each equal-width bin in coloured points and regression lines for each set of quantiles in correspondingly coloured lines. **Figure S5:** Scaling of rainfall event maximum intensity with 3-h pre-event dewpoint temperature for all-raingauges, regional rain gauges and CPM present-day and future climates. Rainfall events are shown as grey points, with fitted quantiles shown of 50%, 95% and 99% for each equal-width bin in coloured points and regression lines for each set of quantiles in correspondingly coloured lines. **Figure S6:** Scaling of rainfall event PW_{50} with 3-h pre-event air temperature for all-raingauges, regional rain gauges and CPM present-day and future climates. Rainfall events are shown as grey points, with fitted quantiles shown from 10% to 90% at regular 20% intervals for each equal-width bin in coloured points and regression lines for each set of quantiles in correspondingly coloured lines. **Figure S7:** Scaling of rainfall event PW_{50} with 3-h pre-event dewpoint temperature for all-raingauges, regional rain gauges and CPM present-day and future climates. Rainfall events are shown as grey points, with fitted quantiles shown from 10% to 90% at regular 20% intervals for each equal-width bin in coloured points and regression lines for each set of quantiles in correspondingly coloured lines. **Figure S8:** Scaling of rainfall event D_{50} with 3-h pre-event air temperature for all-raingauges, regional rain gauges and CPM present-day and future climates. Rainfall events are shown as grey points, with fitted quantiles shown from 10% to 90% at regular 20% intervals for each equal-width bin in coloured points and regression lines for each set of quantiles in correspondingly coloured lines. **Figure S9:** Scaling of rainfall event D_{50} with 3-h pre-event dewpoint temperature for all-raingauges, regional rain gauges and CPM present-day and future climates. Rainfall events are shown as grey points, with fitted quantiles shown from 10% to 90% at regular 20% intervals for each equal-width bin in coloured points and regression lines for each set of quantiles in correspondingly coloured lines.